

Soil warming and nitrogen deposition alter soil organic matter composition at the molecular-level

Oliva Pisani · Serita D. Frey · André J. Simpson · Myrna J. Simpson

Received: 30 June 2014 / Accepted: 21 January 2015 / Published online: 3 February 2015
© Springer International Publishing Switzerland 2015

Abstract Rising temperatures and nitrogen (N) deposition, both aspects of global environmental change, are proposed to alter soil organic matter (SOM) biogeochemistry. For example, increased plant productivity and enhanced microbial decomposition of litter and SOM may reduce soil carbon stocks and fertility. To better understand SOM biogeochemical shifts at the molecular-level, we employed an array of biomarker and nuclear magnetic resonance (NMR) techniques to investigate the composition and degradation of SOM components in the forest floor and mineral soil horizons of warmed (5 °C above average soil temperature) and N fertilized (5 g m⁻² year⁻¹ N applied in the growing season) plots from the soil warming × nitrogen addition study at the Harvard Forest, MA, USA. Biomarker analyses indicated increased plant-derived inputs into

the forest floor under N fertilization. Soil warming promoted the decomposition of plant-derived aliphatic and cyclic compounds in the forest floor. Cutin degradation was observed in the heated forest floor which also exhibited relatively higher microbial activity. Lignin oxidation was also observed but was most pronounced in the mineral horizon of the heated plots. These results suggest that continued soil warming may promote the degradation of lignin- and cuticle-derived SOM. N fertilization also enhanced lignin oxidation but to a lesser extent likely due to a decline in microbial activity. ¹H NMR spectra of the mineral soils revealed enrichment of plant-derived alkyl structures and microbial-derived organic matter with both soil warming and N fertilization. Overall, this study shows that the decomposition and accumulation of molecularly distinct SOM components occurs with soil warming and N amendment and may subsequently alter soil biogeochemical cycling.

Responsible Editor: Sharon A. Billings.

Electronic supplementary material The online version of this article (doi:10.1007/s10533-015-0073-8) contains supplementary material, which is available to authorized users.

O. Pisani · A. J. Simpson · M. J. Simpson (✉)
Department of Physical and Environmental Sciences,
University of Toronto, 1265 Military Trail, Toronto,
ON M1C 1A4, Canada
e-mail: myrna.simpson@utoronto.ca

S. D. Frey
Department of Natural Resources and the Environment,
University of New Hampshire, Durham, NH 03824, USA

Keywords Lignin · Cutin · Suberin · Soil organic matter turnover · Biomarkers · Nuclear magnetic resonance

Introduction

Soil organic matter (SOM) is a heterogeneous mixture of biologically-derived material present at different stages of oxidation (Baldock and Skjemstad 2000).

SOM contains about twice the concentration of carbon than the atmosphere and is an important component of the global carbon cycle (Batjes 1996; Schlesinger and Andrews 2000). SOM sustains microbial, plant and animal life through the retention of water and nutrients (Davidson and Janssens 2006; Trumbore and Czimczik 2008) and plays an essential role in the maintenance of soil fertility and agricultural sustainability (Lal 2004). The amount of carbon stored in soil is highly dependent on the complex interplay between different stabilization mechanisms that combine chemical, physical and biological interactions within the soil matrix (Kögel-Knabner et al. 2008; Schmidt et al. 2011). However, how these stabilization mechanisms will respond to global environmental change such as rising temperatures and nitrogen (N) deposition are still not fully understood.

By the year 2100, the mean global temperature is projected to increase by 0.3–6.4 °C (IPCC 2007). Over the same period, the deposition of reactive N, from fossil fuel combustion and agricultural fertilizer application, into terrestrial ecosystems is predicted to double (Galloway et al. 2004). These aspects of environmental change may alter biogeochemical processes in terrestrial ecosystems such as plant primary productivity (Shaver et al. 2000; Melillo et al. 2011), microbial community structure (Frey et al. 2008), soil respiration and N mineralization (Melillo et al. 2002; Contosta et al. 2011), litter decomposition and nutrient cycling (Berg et al. 1993; Knorr et al. 2005; Zhang et al. 2008). Rising temperatures are likely to change SOM composition through vegetation and microbial shifts (Feng et al. 2008) and by changing the soil microbial community composition and microbial decomposition patterns of SOM (Feng et al. 2008; Frey et al. 2008, 2013). For example, Feng et al. (2008) showed that 14 months of soil warming resulted in accelerated lignin decomposition, accumulation of cutin-derived SOM, increased microbial activity and a decline in labile SOM. Nitrogen fertilization is believed to promote plant growth (Vitousek et al. 2002) and microbial decomposition in N-limited environments (Knorr et al. 2005). N fertilization may result in modification to the soil microbial community and plant detrital inputs which can subsequently alter SOM decomposition patterns (Frey et al. 2004; Feng et al. 2010). Frey et al. (2014) reported that chronic N fertilization reduced SOM decomposition and altered SOM chemistry.

Based on these studies, we hypothesize that soil warming will reduce labile SOM constituents and alter the long-term stability of lignin and recalcitrant SOM. We also hypothesize that N addition may reduce SOM decomposition of labile and recalcitrant components whereas simultaneous warming + N will result in unique shifts in SOM composition that differs from either warming or N addition alone. The objective of this study was to combine two molecular-level methods, biomarker analyses and nuclear magnetic resonance (NMR) spectroscopy, to assess changes in the composition and degradation of SOM in response to soil warming and N fertilization. Soil samples were collected from the soil warming × nitrogen addition study located at the Harvard Forest Long-Term Ecological Research (LTER) site in Massachusetts, USA after 4 years of manipulation. We employed biomarker extraction techniques to study the sources and stage of SOM decomposition which included: solvent extraction (free lipids), base hydrolysis (cutin- and suberin-derived compounds), copper (II) oxide (CuO) oxidation (lignin-derived phenols), and phospholipid fatty acid (PLFA) analysis for the identification of microbial community composition and activity (Feng and Simpson 2011). NMR was also employed to gain information about the composition of whole soils and base soluble SOM. The combination of biomarker analyses and NMR methods provides detailed insight into SOM composition and can aid in unraveling ecosystem functions with environmental change (Simpson et al. 2008; Feng and Simpson 2011).

Materials and methods

Site description and sample collection

Samples were collected from the Soil Warming × Nitrogen Addition Study plots located at the Prospect Hill Tract of the Harvard Forest LTER (<http://harvardforest.fas.harvard.edu>) site in Petersham, Massachusetts, USA (42°50'N, 72°18'W) after 4 years of treatment. The forest is composed of even-aged, mixed hardwoods, such as red oak (*Quercus rubra*), black oak (*Quercus velutina*), red maple (*Acer rubrum*), striped maple (*Acer pensylvanicum*), American beech (*Fagus grandifolia*), white birch (*Betula papyrifera*) and American

chestnut (*Castanea dentata*). The soils are of the Gloucester series (fine loamy, mixed, mesic typic dystrochrept; Peterjohn et al. 1994). The mean annual air temperature at the Harvard Forest is 7 °C, with summer and winter temperatures as high as 32 °C and as low as –25 °C, respectively. The average total annual precipitation, including water equivalent of snow, is 1,100 mm. Mean annual snowfall occurs primarily from December through February (Contosta et al. 2011).

The experiment is composed of twenty-four 3 m × 3 m plots that have been randomly assigned one of four treatments (six replicate plots per treatment): control, warming, nitrogen and warming + nitrogen. The soil temperature in the warming and warming + nitrogen plots is continuously elevated 5 °C above ambient with the use of buried heating cables placed 10 cm below the soil surface and spaced 20 cm apart. The cables were installed in October 2005 and activated in August 2006 to allow system recovery. Nitrogen additions to the nitrogen and warming + nitrogen plots were also initiated in August 2006 and N is applied in equal doses during the growing season (May–October) as an aqueous solution of NH_4NO_3 ($5 \text{ g N m}^{-2} \text{ year}^{-1}$). This fertilization rate is about eight times that of ambient N deposition at the Harvard Forest ($0.66 \text{ g N m}^{-2} \text{ year}^{-1}$; Munger et al. 1998).

Soil samples were collected in October 2010. One 10 cm core was collected from each plot and separated into forest floor and mineral horizon fractions. Leaf litter and roots were collected from the Harvard Forest and placed in clean bags. All the samples were air-dried and ground prior to analysis. The organic carbon and N content of the plant and soil samples was measured using combustion analysis with a Carlo Erba 1500 elemental analyzer (Carlo Erba, Milan, Italy). The organic carbon and N content of the forest floor and the mineral horizon soils did not change markedly with soil warming and N fertilization (Table S1 in ESM).

Sequential biomarker extractions

Sequential biomarker extractions (solvent extraction, base hydrolysis and CuO oxidation) were conducted in duplicate on the plant and soil samples to isolate free lipids, cutin- and suberin-derived ester-bound lipids and lignin-derived phenols, respectively (Hedges and

Mann 1979; Goñi and Hedges 1990a; Otto and Simpson 2007). Samples (~1–10 g, depending on the organic carbon content) were Soxhlet extracted in duplicate with 150 ml of dichloromethane:methanol (DCM:MeOH; 1:1; v/v) for 24 h and the resulting extract was concentrated by rotary evaporation, transferred to 2 ml vials and dried under a stream of N_2 gas. The air-dried residues (~0.2–10 g) were heated at 100 °C for 3 h in Teflon-lined bombs with 20 ml of 1 M methanolic KOH for the extraction of hydrolysable lipids (Goñi and Hedges 1990a; Otto and Simpson 2006a). The extracts were acidified to pH 1 by addition of 6 M HCl and the hydrolysable lipids were recovered by liquid–liquid extraction with diethyl ether. Anhydrous Na_2SO_4 was added to the ether phase to remove water and the ether extracts were concentrated by rotary evaporation, transferred to 2 ml vials and dried under N_2 gas. The soil residues were air dried and further extracted (~0.2–0.5 g) with 1 g CuO, 100 mg ammonium iron (II) sulfate hexahydrate [$\text{Fe}(\text{NH}_4)_2(\text{SO}_4)_2 \cdot 6\text{H}_2\text{O}$] and 15 ml of 2 M NaOH, purged with N_2 gas and heated in an oven set at 170 °C for 2.5 h in Teflon-lined bombs to isolate lignin-derived phenols (Hedges and Mann 1979; Otto and Simpson 2006b). The extracts were acidified to pH 1 by addition of 6 M HCl and kept in the dark at room temperature for 1 h to prevent reactions of cinnamic acids. Lignin-derived phenols were isolated by liquid–liquid extraction with diethyl ether, concentrated by rotary evaporation, transferred to 2 ml vials and dried under a stream of N_2 gas.

Phospholipid fatty acid analysis

To assess the microbial activity and community composition, PLFA biomarkers were extracted in duplicate from the soil samples by a modified Bligh–Dyer method (Frostegård and Bååth 1996; Feng and Simpson 2009). Freeze-dried soil samples (~0.5–0.75 g) were extracted with 30 ml of a single phase mixture (1:2:0.8, v:v:v) of chloroform (CHCl_3), methanol (CH_3OH) and citrate buffer (0.15 M, pH 4) by shaking for 24 h. The CHCl_3 phase was collected by centrifugation and fractionated into neutral, glyco- and polar lipids with 10 ml of CHCl_3 , 20 ml of acetone and 10 ml of CH_3OH , respectively by silica column chromatography. The PLFAs contained in the polar lipid fraction, were converted to fatty acid methyl esters (FAMES) by a mild alkaline

methanolysis reaction (37 °C for 15 min), recovered with a hexane:CHCl₃ mixture (4:1, v:v), transferred to 2 ml vials and dried under a stream of N₂ gas.

Fatty acids were designated according to the standard PLFA nomenclature (Guckert et al. 1985) which is based on the number of carbon atoms and the number of double bonds followed by the position of the double bond from the methyl end of the molecule. The $\omega(n)$ indicates that the first double bond starts on the n th carbon from the aliphatic end of the FAME. The prefixes *i*- and *a*- refer to *iso*- and *anteiso*-branched fatty acids, respectively. Other methyl-branching is indicated as the position from the carboxylic acid end (i.e., 10Me18:0). The *cy*- designation indicates cyclopropane fatty acids. The total active microbial biomass was calculated by taking the sum of all PLFAs (C₁₄–C₂₀). The sum was taken for PLFAs specific to fungi (18:2 ω 6,9), actinomycetes (10Me18:0), gram-negative bacteria (16:1 ω 7, *cy*17:0, 18:1 ω 7 and *cy*19:0) and gram-positive bacteria (*i*14:0, *i*15:0, *a*15:0, *i*16:0, *a*16:0, *i*17:0 and *a*17:0). To assess microbial community changes due to soil warming and N fertilization, the ratio of fungal to bacterial PLFAs (the sum of gram-negative and gram-positive bacteria; fungal/bacterial) and the ratio of gram-negative to gram-positive bacterial PLFAs (gram-negative/gram-positive) were calculated.

Quantification by gas chromatography–mass spectrometry (GC–MS)

The solvent and CuO extracts were converted to trimethylsilyl (TMS) derivatives by reaction with 100 μ l of *N,O*-Bis(trimethylsilyl)trifluoroacetamide (BSTFA) and 10 μ l of anhydrous pyridine at 70 °C for 1.5 h. The extracts from base hydrolysis were first derivatized with *N,N*-dimethylformamide dimethyl acetal (Thenot et al. 1972) and then with BSTFA and pyridine. After cooling, hexane was added to dilute the extracts prior to GC–MS analysis. Samples were run on an Agilent 6890N GC coupled to an Agilent 5973 quadrupole mass selective detector. The GC was fitted with a HP5-MS fused silica capillary column (30 m \times 0.25 mm i.d., 0.25 μ m film thickness). The GC oven temperature was held at 65 °C for 2 min, increased to 300 °C at a rate of 6 °C min⁻¹ with a final isothermal hold of 20 min. A 1 μ l aliquot of sample extract was injected using an Agilent 7683 autosampler with the injector temperature set to

280 °C. Helium was used as the carrier gas with a flow rate of 1.2 ml min⁻¹. The mass spectrometer was operated in electron impact (EI) mode with ionization energy of 70 eV and scanned from 50 to 650 Da. Data were acquired and processed using the MSD Productivity ChemStation software (v E.02.02). Individual compounds were identified by comparison of mass spectra with those of authentic standards, NIST and Wiley275 MS library data, literature and interpretation of fragmentation patterns. Quantification was performed using external standards: tetracosane, 1-docosanol (as TMS ester), methyl tricosanoate and ergosterol (as TMS ester) for the solvent-extractable lipids; methyl tricosanoate for the hydrolysable lipids; vanillic acid and vanillin (as TMS esters) for the CuO products; oleic acid methyl ester for the PLFAs. The relative standard deviation associated with the employed method has been reported to be ~5 % (Otto and Simpson 2007).

Solid- and solution-state nuclear magnetic resonance spectroscopy

In preparation for solid-state ¹³C cross polarization with magic angle spinning (CPMAS) NMR, freeze-dried mineral horizon soil samples (~90 g) were repeatedly treated with hydrofluoric acid (HF; 10 %) to concentrate the organic matter and to remove paramagnetic minerals that can be problematic during acquisition (Schmidt et al. 1997; Simpson et al. 2012). The treatment with HF has been shown to maintain the overall organic matter composition (Rumpel et al. 2006). After treatment with HF, the samples were rinsed with deionized water to remove excess salts and freeze-dried. Approximately 100 mg of whole (forest floor) and HF-treated (mineral horizon) sample was packed into a 4 mm zirconium rotor with a Kel-F cap. The spectra were acquired on a 500 MHz Bruker BioSpin Avance III spectrometer (Bruker BioSpin, Rheinstetten, Germany) equipped with a 4 mm H–X MAS probe and using a ramp-CP pulse program (Conte et al. 2004) with a spinning rate of 13 kHz and a ramp-CP contact time of 1 ms and 1 s recycle delay. The spectra were processed using a zero filling factor of 2 and line broadening of 100 Hz. The spectra were integrated into four chemical shift regions corresponding to: alkyl (0–50 ppm), *O*-alkyl (50–110 ppm), aromatic and phenolic (110–165 ppm), and carboxyl and carbonyl carbon (165–215 ppm; Baldock et al.

1992; Simpson et al. 2008). All chemical shifts were calibrated using an external glycine standard and the total NMR signal (0–215 ppm) was normalized to 100 % for comparisons of the relative contents of each type of carbon. Alkyl/*O*-alkyl ratios were calculated by dividing the areas of the alkyl and the *O*-alkyl regions of the spectra (Baldock et al. 1992; Simpson et al. 2008).

For solution-state NMR analysis, the whole (forest floor, ~10 g) and HF-treated (mineral horizon, ~20 g) soil samples were extracted with 0.1 M NaOH, filtered with 0.22 µm membrane filters (Millipore, Durapore®), cation-exchanged using Amberjet 1200H ion exchange resin and freeze-dried. The base-soluble extracts (~100 mg) were further dried over P₂O₅ to remove residual water, re-dissolved in 1 ml of DMSO-*d*₆ and transferred to a 5 mm NMR tube for analysis. The solution-state NMR spectra were acquired with a Bruker BioSpin Avance 500 MHz spectrometer equipped with a 5 mm QXI probe fitted with an actively shielded Z-gradient at 298 K. One-dimensional (1-D) solution-state ¹H NMR experiments were acquired using 64 scans and 16,384 time domain points with a recycle delay of 2 s. 1-D diffusion edited (DE) ¹H NMR experiments were performed using a bipolar pulse longitudinal encode-decode sequence with 64 scans, 16,384 time domain points, a diffusion time of 200 ms and 2.5 ms encoding and decoding gradients at 53.5 gauss cm⁻¹. All the solution-state 1-D ¹H NMR spectra were processed using a zero-filling factor of 2 and line broadening of 1 Hz. Two-dimensional (2-D) correlation spectroscopy (COSY) spectra were acquired using a 45° read pulse with 128 scans collected for each of the 196 increments in the F1 dimension and 128 time domain points collected in the F2 dimension. Heteronuclear single quantum correlation (HSQC) spectra were collected in the phase-sensitive mode using Echo/Antiecho-TPPI gradient selection and an average ¹J ¹H–¹³C of 145 Hz. Scans (512) were collected for each of the 64 increments in the F1 dimension and 1,024 time domain points collected in the F2 dimension with a recycle delay of 1 s. Heteronuclear multiple bond connectivity (HMBC) spectra were collected in the phase-sensitive mode using Echo/Antiecho-TPPI gradient selection and a relaxation optimized delay of 25 ms for the evolution of long-range couplings. Scans (256) were collected for the 96 increments in the F1 dimension and 2,048

time domain points collected in the F2 dimension with a recycle delay of 1 s. All the 2-D solution-state NMR spectra were processed by multiplying the F2 dimensions by an exponential function corresponding to a 15 Hz line broadening. The F1 dimensions were processed using a sine-squared function with a π/2 phase-shift and a zero-filling factor of 2. Chemical shift assignments are based on previously published data (Clemente et al. 2012; Deshmukh et al. 2003, 2007; Kelleher and Simpson 2006; Pautler et al. 2013; Simpson et al. 2001, 2004, 2007; Woods et al. 2011) and confirmed by 2-D NMR experiments and NMR spectral predictions using Advanced Chemistry Development's ACD/SpecManager and ACD/2-D NMR Predictor using neural network prediction algorithms.

Statistical analyses

A one way analysis of variance (ANOVA) using the Holm–Sidak as a multiple comparison test was used to compare the concentration of SOM components between treatments (control, warming, nitrogen and warming + nitrogen) of the forest floor and mineral horizons. The statistical experimental unit was taken as each treatment plot (six plots per treatment; duplicate biomarker analysis, *n* = 12 per sample per treatment). A difference was considered significant at the level of *p* ≤ 0.05. Statistical analyses were performed using SigmaPlot (v 11.0).

Results

Organic matter biomarkers

Molecular fingerprint of the leaf litter, roots, and soil samples from the Control plots

The solvent extracts of the plant material, forest floor and mineral horizon Control soils contained a series of aliphatic lipids (*n*-alkanes, *n*-alkanols, *n*-alkanoic acids and *n*-alkane dioic acids), cyclic compounds (triterpenoids and steroids) and carbohydrates (Tables S1 and S2 in ESM). Long-chain homologues (≥C₂₀) of aliphatic lipids are characteristic of epicuticular waxes of higher plants (Simoneit 2005) whereas short-chain compounds (<C₂₀) originate from soil microbes such as fungi and bacteria (Lichtfouse et al. 1995; Otto

and Simpson 2005). Short-chain lipids have been shown to preferentially degrade compared to their long-chain counterparts (Schulten and Schnitzer 1990). To determine the source and extent of degradation of different free lipid classes, the ratio of short- to long-chain aliphatic lipids (SCA/LCA) and the ratio of the total concentration of glucose to LCA (glucose/LCA) were calculated (Fig. 1a). An expanded plot (Fig. 1b) shows that these ratios were higher for the mineral compared to the forest floor soils.

We also observed stigmasterol and β -sitosterol, which are phytosterols commonly found in vascular plants (Simoneit 2005). The sterones stigmastan-3-one and stigmasta-3,5-diene-7-one are degradation products of sterols and are indicative of SOM biodegradation (Mackenzie et al. 1982; Otto and Simpson 2005) and this ratio (Fig. 1c) shows that the plant material has a unique signature relative to the

soil samples. The aliphatic to cyclic compound ratio (aliphatic/cyclic; Fig. 1c) can also be used to assess the degradation stage of SOM (Otto and Simpson 2005; Pisani et al. 2013) and reveals that cyclic compounds are more abundant in the plant material compared to the Control soils. We observed a lower aliphatic/cyclic ratio (Fig. 1d) for the mineral compared to the forest floor soil, suggesting the preservation of cyclic compounds in the mineral soil. Simple carbohydrates, such as glucose and mannose which can originate from animals, plants and soil microbes (Simoneit et al. 2004), were the most abundant solvent-extractable compounds of the plant material and were present at similar concentrations in both the leaf litter and root samples (Table S1 in ESM). Trehalose is a reserve carbohydrate that functions as a stress protector in fungi and bacteria (Koide et al. 2000) and was not detected in the leaf litter, but was

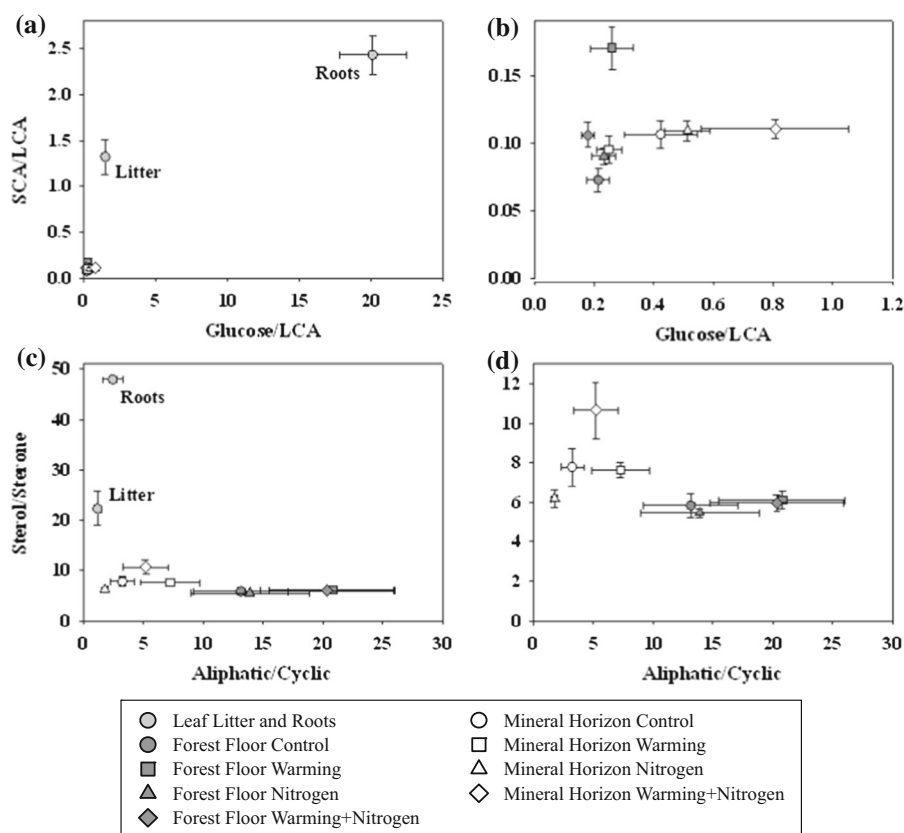


Fig. 1 Solvent-extractable (free lipids) SOM composition and degradation trends for the leaf litter, plant roots, forest floor and mineral horizon soils. **a** The ratio of short-chain (SCA; $<C_{20}$) to long-chain aliphatic lipids (LCA; $\geq C_{20}$) and glucose/LCA.

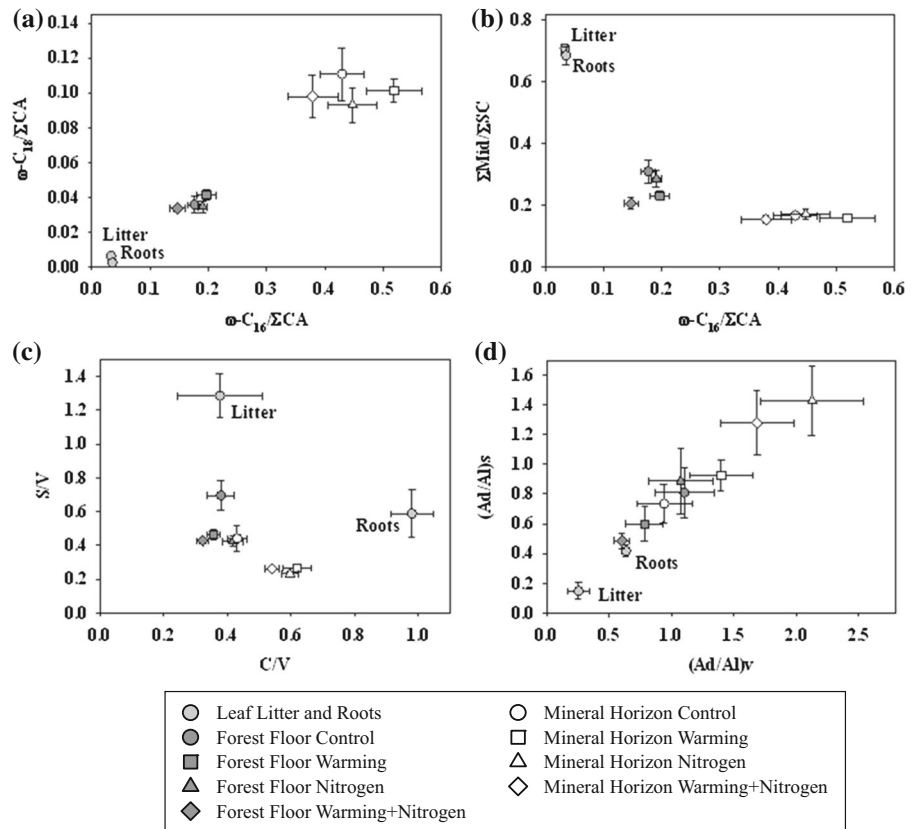
b Expanded plot excluding leaf litter and roots. **c** Sterol/sterone (Σ stigmasterol and sitosterol/ Σ stigmastan-3-one and stigmasta-3,5-dien-7-one) and aliphatic/cyclic (Σ aliphatic/ Σ cyclic compounds). **d** Expanded plot excluding leaf litter and roots

present in the roots. The concentration of simple carbohydrates decreased from the source vegetation to the forest floor and mineral horizon soil.

The ester-bound compounds released after base hydrolysis included a series of aliphatic lipids (*n*-alkanols, *n*-alkanoic acids, branched alkanolic acids, *n*-alkane dioic acids, ω -hydroxyalkanoic acids, mono-, di- and tri-hydroxyalkanoic and epoxy acids and α -hydroxyalkanoic acids), benzenes (*p*-hydroxy benzoic acid) and phenols (vanillin, acetovanillone, vanillic acid, syringaldehyde, acetosyringone, syringic acid, *p*-coumaric acid and ferulic acid) which can be attributed to suberin, cutin or both polymers (Kolattukudy 1980; Otto and Simpson 2006a; Table S3 in ESM). Based on the occurrence of these compounds in suberin or cutin, several biomarkers have been developed to differentiate between cutin- and suberin-derived inputs to soils (Otto and Simpson 2006a; Table S1 in ESM). Suberin-derived compounds (ΣS) were more abundant in plant roots while cutin-derived compounds (ΣC) were more abundant in

the leaf litter, resulting in distinct suberin/cutin ratios. In the forest floor Control plot, ΣC was lower compared to the leaf litter and was much lower in the mineral horizon, suggesting cutin degradation with soil depth or a shift from aboveground to belowground organic matter inputs. Suberin-derived inputs were higher in the mineral compared to the forest floor soils as indicated by a higher ΣS and suberin/cutin ratio (Table S1 in ESM). The sum of suberin and cutin acids (ΣSC) decreased from the plant to the soil samples suggesting that ester-bound aliphatic lipids derived from roots and leaves are degraded with deposition. Cutin degradation can be estimated using a plot of the ratio of ω -C₁₆ and ω -C₁₈ hydroxyalkanoic acids to the total concentration of cutin acids (ΣCA) because cutin-derived mid-chain-substituted hydroxy and epoxy acids are preferentially degraded (Gofni and Hedges 1990b; Otto and Simpson 2006a). Such a plot (Fig. 2a) shows that both of these ratios increased from the plant samples and with soil depth. A similar trend was observed for the ratio of mid-chain-

Fig. 2 Cutin, suberin and lignin-derived phenol degradation trends for the leaf litter, plant roots, forest floor and mineral horizon soils. **a** The ratio of C₁₈ and C₁₆ ω -hydroxyalkanoic acids to the total concentration of cutin acids ($\Sigma CA = \Sigma C_{14}-C_{18}$ mid-chain hydroxy and epoxy acids + ΣC_{16} and C₁₈ ω -hydroxyalkanoic and α,ω -dioic acids). **b** The ratio of mid-chain cutin acids ($\Sigma Mid = \Sigma C_{14}-C_{18}$ mid-chain hydroxy and epoxy acids) to the total suberin and cutin acids ($\Sigma SC = \text{sum of all aliphatic acids derived from suberin and cutin}$). **c** Syringyl/vanillyl (*S/V*) and cinnamyl/vanillyl (*C/V*). **d** Acid to aldehyde ratios for syringyl (*Ad/Al*)_s and vanillyl (*Ad/Al*)_v phenols



substituted acids to the total cutin and suberin acids ($\Sigma\text{Mid}/\Sigma\text{SC}$; Fig. 2b).

The CuO oxidation products included several lignin monomers of the vanillyl (vanillin, acetovanillone, vanillic acid and vanillyl glyoxylic acid), syringyl (syringaldehyde, acetosyringone, syringic acid and syringyl glyoxylic acid) and cinnamyl (hydrocinnamic acid, 3-methoxycinnamic acid, *p*-coumaric acid, ferulic acid, 3,4-dihydroxycinnamic acid and sinapic acid) groups, benzenes (benzoic acid, *p*-hydroxybenzaldehyde, *p*-hydroxybenzoic acid, 3,5-dihydroxybenzoic acid, 3,4-dihydroxybenzoic acid and 3,4,5-trihydroxybenzoic acid) and a small concentration of lignin dimers (5,5'-dimers, β ,1-diketone dimers and α ,2-methyl dimers; Table S1 in ESM). The composition of lignin-derived phenols is characteristic of major plant groups because gymnosperm wood contains only vanillyl derivatives while angiosperm wood contains approximately equal quantities of vanillyl and syringyl derivatives (Hedges and Mann 1979). In addition, the non-woody tissues of vascular plants (e.g., conifer needles, grass, angiosperm leaves) contain cinnamyl units that are part of the lignin macromolecule or the lignocellulose complex (Lam et al. 2001). As such, a plot of the ratios of syringyl to vanillyl (S/V) and cinnamyl to vanillyl (C/V) monomers can be used to assess the botanical origin of lignin in soils and shows that the leaf litter from the Harvard Forest is dominated by syringyl units resulting in an S/V of 1.28 ± 0.13 (Fig. 2c). The roots contained similar concentrations of vanillyl and cinnamyl monomers and had a C/V of 0.98 ± 0.07 . Vanillyl units were the most abundant monomers (S/V of 0.69 ± 0.09) in the forest floor (Fig. 2c) and were in higher concentrations relative to aboveground litter. Vanillyl units were also the most abundant monomers in the mineral soils (S/V of 0.44 ± 0.08), but in lower concentration compared to the forest floor soils. The lignin dimers were not detected in the plant samples and were only found in small concentrations in the soil samples (Table S1 in ESM). Progressive lignin degradation is also reflected by elevated ratios of lignin-derived phenolic acids and their corresponding aldehydes (Ad/Al) for both syringyl and vanillyl units (Hedges et al. 1988; Otto and Simpson 2006b). These ratios are typically 0.1–0.2 for fresh angiosperm and conifer wood and 0.2–1.6 for non-woody tissues such as leaves, needles and grasses (Hedges and Mann 1979; Hedges et al. 1988). The litter and root samples had lower Ad/Al ratios compared to the soils (Fig. 2d).

However, no difference in Ad/Al was observed between the forest floor and mineral Control soils.

Profiles of PLFAs are typically used to study microbial activity and community composition in soil environments because PLFAs are only found in viable cells and are characteristic of living microbes (Frostegård and Bååth 1996). PLFA analysis showed that the forest floor and mineral soils have unique PLFA signatures (Table S1 in ESM). The fungal/bacterial ratio indicated that fungal activity is higher in the forest floor compared to the mineral soil. The gram-negative/gram-positive bacterial ratio was similar in both the forest floor and mineral soils.

Molecular composition of SOM in warmed soils

Soil warming increased the concentration of short-chain free aliphatic lipids ($p \leq 0.05$; Table S1 in ESM) in the forest floor (elevated SCA/LCA ratio) but not in the mineral horizon (Fig. 1b). The sterol/sterone ratio did not change with soil warming (Fig. 1d). The aliphatic/cyclic lipid ratio did not change in the forest floor, but increased in the heated mineral soil (Fig. 1d). Figure 3 shows the percent relative changes in biomarker concentrations and reveals the decrease in both aliphatic and cyclic lipids and a slight increase in simple carbohydrates in the forest floor. Soil warming caused a decrease in aliphatic lipids and simple carbohydrates in the mineral horizon (Fig. 3b) and only a small change in cyclic lipids.

The total suberin- and cutin-derived compounds did not change significantly in the forest floor with warming but there was a slight increase in ΣS and suberin/cutin ratio (Table S1 in ESM; Fig. 3a). In the mineral horizons, warming caused a significant decrease in ΣS , ΣC and in the total concentration of bound lipids ($p \leq 0.05$; Table S1 in ESM; Fig. 3b) and an increase in the suberin/cutin ratio. Soil warming also resulted in an increase in cutin degradation in the mineral soils (elevated $\omega\text{-C}_{16}/\Sigma\text{CA}$ ratio; Fig. 2a). In the forest floor, a decrease in the $\Sigma\text{Mid}/\Sigma\text{SC}$ ratio also indicates enhanced cutin degradation with soil warming (Fig. 2b).

The concentration of lignin-derived phenols did not change significantly in the forest floor with soil warming (Table S1 in ESM; Fig. 3a). However, the S/V decreased (Fig. 2c) suggesting the preferential degradation of syringyl monomers with soil warming. Lignin oxidation did not increase with soil warming

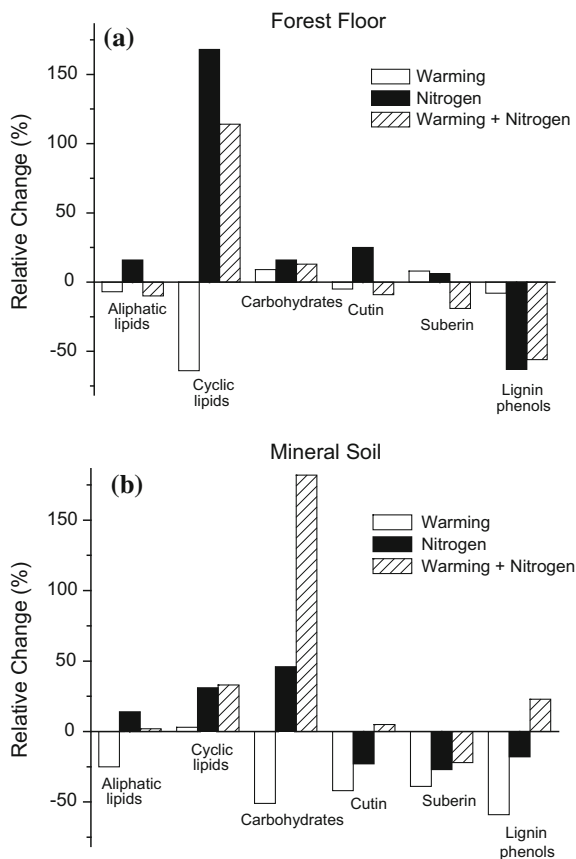


Fig. 3 Percent changes (relative to the control) in the concentration of major SOM molecular components in the forest floor and mineral horizon soil samples after 4 years of soil warming, N fertilization and both treatments. SOM components were calculated from biomarker analyses and include: aliphatic lipids, cyclic lipids, simple carbohydrates (galactose, glucose, and mannose), cutin-derived bound lipids, suberin-derived bound lipids and lignin-derived phenols. Biomarker concentrations for all samples are listed in the supplementary material

and the Ad/Al ratios of the heated forest floor soil were lower compared to the control (Fig. 2d). In the mineral soils heating caused a significant decrease in the concentration of all lignin-derived phenols ($p \leq 0.05$; Table S1 in ESM; Fig. 3b) and resulted in a lower S/V compared to the mineral Control soil (Fig. 2c). However, the C/V of the heated mineral soil increased compared to the Control. Lignin oxidation and Ad/Al ratios also increased in the heated mineral soil (Fig. 2d). After 4 years of soil warming, the total PLFAs of the forest floor increased (Table S1 in ESM). In particular, there was a significant increase in the concentration of gram-positive bacteria and actinomycetes ($p \leq 0.05$) suggesting increased microbial

activity. The microbial community composition of the forest floor shifted towards gram-positive bacteria as indicated by a lower gram-negative/gram-positive bacterial ratio. No significant change in microbial PLFAs and in microbial community composition was observed in the heated mineral soils.

Molecular composition of SOM in N fertilized soils

Alteration of SOM molecular components after 4 years of N fertilization were less pronounced than changes observed with soil warming. There was no significant change in the concentration of free lipid compounds in both the forest floor and mineral horizon soils with N fertilization (Table S1 in ESM) but the concentration of aliphatic and cyclic components in both the forest floor (Fig. 3a) and mineral soils increased (Fig. 3b). Nitrogen fertilization also caused an increase in simple carbohydrates in the mineral soils, but these changes were not statistically significant. The SCA/LCA ratio in the forest floor increased marginally with N fertilization (Fig. 1b). The sterol/sterone ratio did not change with N fertilization in the forest floor, but it decreased in the mineral soils (Fig. 1d), suggesting enhanced sterol degradation. The aliphatic/cyclic ratio did not change with N fertilization. The concentration of suberin- and cutin-derived compounds showed no significant change in the forest floor and mineral soils after 4 years of N fertilization (Table S1 in ESM) although there was a decrease in ΣS in the mineral soil (Fig. 3b). Cutin degradation was not altered by N fertilization as there were no changes in either the $\omega\text{-C}_{16}/\Sigma CA$ and $\Sigma Mid/\Sigma SC$ ratios for both the forest floor and mineral horizon soils (Fig. 2a, b).

The lignin-derived phenols decreased with N fertilization. The concentration of syringyl phenols and total lignin monomers decreased in the forest floor ($p \leq 0.05$; Table S1 in ESM; Fig. 3a). This resulted in a lower S/V ratio compared to the Control soil (Fig. 2c), suggesting the preferential degradation of syringyl units. However, the Ad/Al ratio of the forest floor did not change after 4 years of N fertilization (Fig. 2d). In the mineral horizon, N fertilization caused a significant decrease only for the syringyl units ($p \leq 0.05$; Table S1 in ESM). This is also shown by a lower S/V value (Fig. 2c) and an increased Ad/Al ratio (Fig. 2d). The microbial PLFAs of the forest floor did not change with N fertilization although there appeared to be a shift in the microbial community

composition towards gram-negative bacteria (Table S1 in ESM). N fertilization caused a reduction in total PLFAs and a shift in microbial composition towards gram-negative bacteria ($p \leq 0.05$; Table S1 in ESM) in the mineral soil horizons.

Molecular composition of SOM in warmed and N fertilized soils

The combination of soil warming and N fertilization did not cause any significant changes in the concentration of free lipids in the forest floor (Table S1 in ESM). However, a small decrease in the total concentration of aliphatic lipids and an increase in cyclic compounds and small carbohydrates (Fig. 3a), along with an increase in the SCA/LCA ratio (Fig. 1b) was observed. In the mineral horizon, the combination of both treatments caused a small increase in free lipids although these changes were not statistically significant. The glucose/LCA (Fig. 1b) and the sterol/sterone ratios increased in the mineral soils (Fig. 1d).

The concentration of suberin- and cutin-derived compounds significantly decreased in the forest floor ($p \leq 0.05$; Table S1 in ESM) but did not change in the mineral soil. The combination of both treatments did not influence cutin degradation in either the forest floor or mineral soils (Figs. 2a, b, 3). In both the forest floor and mineral soils, a decrease in ΣS was observed, although this change was not statistically significant (Table S1 in ESM; Fig. 3e, f).

The lignin-derived phenols decreased with both treatments in the forest floor (Fig. 3a). In particular, monomers of the syringyl group decreased significantly ($p \leq 0.05$; Table S1 in ESM) resulting in a lower S/V ratio (Fig. 2c). However, lignin oxidation and Ad/Al ratios were lower in the heated and fertilized soil compared to the Control (Fig. 2d). In the mineral soils, the combination of both treatments did not cause any significant change in lignin-derived phenol composition (Table S1 in ESM) although an increase was observed in VSC concentrations (Fig. 3b). The S/V of the mineral soils receiving both treatments decreased and the C/V increased (Fig. 2c). Lignin oxidation increased as shown by elevated Ad/Al ratios (Fig. 2d). Finally, the combination of soil warming and N fertilization caused slight changes in the soil microbial community composition with a shift towards fungi in the forest floor (Table S1 in ESM). In the mineral soils there was a small decrease in the total

PLFAs with a significant decrease in the concentration of gram-negative bacteria ($p \leq 0.05$; Table S1 in ESM).

Nuclear magnetic resonance spectroscopy

Solid-state ^{13}C NMR of soil samples

The solid-state ^{13}C NMR spectra (an example of the forest floor and mineral horizon Control soils are shown in Fig. 4) reveal that the forest floor is dominated by *O*-alkyl carbon (Table S4 in ESM) from oxygen and nitrogen-substituted aliphatic constituents found in carbohydrates, peptides and methoxyl carbon found in lignin (Baldock et al. 1992; Simpson et al. 2008). The mineral soil is dominated by alkyl carbon (Table S4 in ESM) originating from cutin, suberin, aliphatic side-chains and lipids (Baldock et al. 1992; Simpson et al. 2008). The aromatic and phenolic signals from lignin and aromatic amino acids in peptides (Baldock et al. 1992; Simpson et al. 2008) were relatively more intense in the mineral soil compared to the forest floor. The signal originating from the carboxyl and carbonyl carbon in fatty acids and amino acids found in peptides (Baldock et al. 1992; Simpson et al. 2008) were relatively more intense in the mineral soil. In the forest floor, the ^{13}C NMR spectra did not show any major differences in the relative percent of different carbon structural units with the various treatments. However, differences were observed in the mineral horizon soils. The signal deriving from alkyl carbon increased with soil warming and decreased with N fertilization as well as with both treatments (Table S4 in ESM). The signal from *O*-alkyl carbon decreased in the heated soils and increased with both soil warming and N fertilization. The signals from aromatic, carboxyl and carbonyl carbons showed a slight increase with all the treatments. The ratio of alkyl/*O*-alkyl carbon is often used to compare the relative stage of degradation of SOM because *O*-alkyl compounds are labile and more easily degraded compared to alkyl compounds, resulting in increased ratios with progressive SOM degradation (Baldock et al. 1992; Simpson et al. 2008; Simpson and Simpson 2012). In the forest floor, this ratio only decreased slightly in the N fertilized soils and in the soils receiving both treatments (Table S4 in ESM). This ratio was higher in the mineral soils and increased in the heated plots. The alkyl/*O*-alkyl ratio decreased

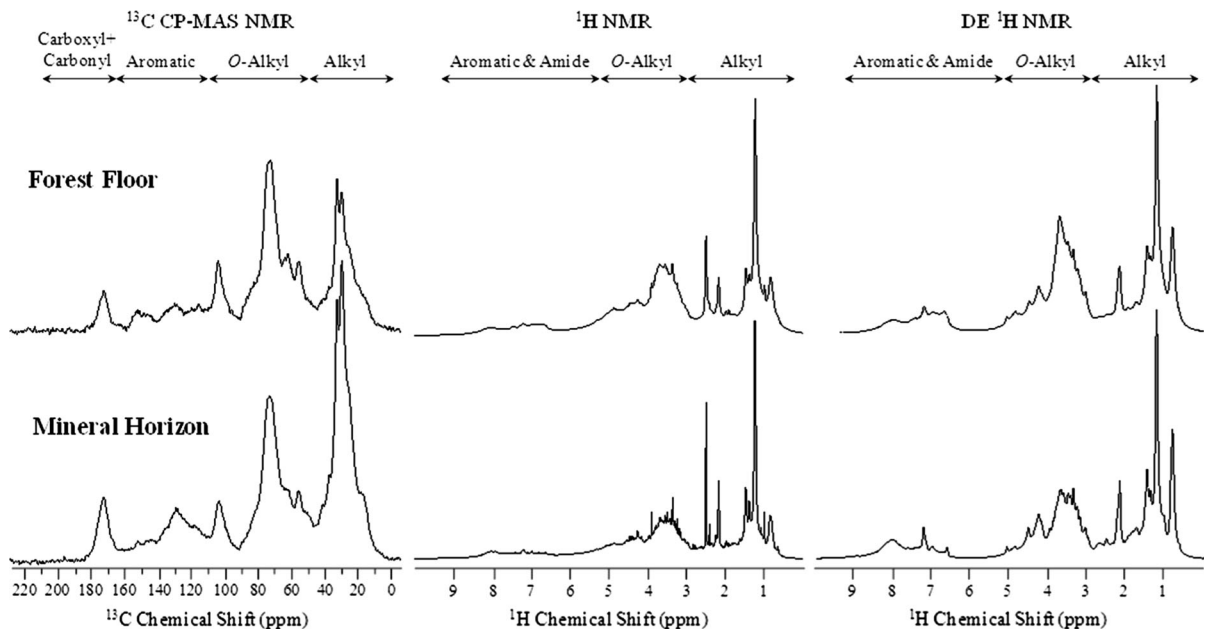


Fig. 4 Examples of solid-state ^{13}C , solution-state 1-D ^1H and diffusion edited (DE) ^1H NMR spectra for the forest floor and mineral horizon Control soils

in the N fertilized mineral soils and in the soils receiving both warming and N fertilization.

1-D solution-state ^1H NMR of base-soluble SOM extracts

The solution-state ^1H NMR spectra of the forest floor and mineral horizon base-soluble extracts indicate that they are dominated by *O*-alkyl components (Table S4 in ESM; Fig. 4) originating from lignin, carbohydrates and peptides (Simpson et al. 2007; Clemente et al. 2012). In the forest floor the alkyl region from cutin and suberin in plants, lipids and amino acid side-chains (Simpson et al. 2007) showed an increase in relative percent after 4 years of N fertilization and with both warming and N fertilization. The relative intensity of the *O*-alkyl region decreased in the heated soils and increased with N fertilization and with both treatments. The signal originating from the α -protons in peptides (Simpson et al. 2007) showed a slight decrease with all treatments. The aromatic signal from lignin, peptides and the amide signal from peptides (Simpson et al. 2007) increased in the heated forest floor soils and decreased in the N fertilized soils. In the mineral soil samples the alkyl signal increased with all the treatments. The *O*-alkyl and the *O*- or *N*-substituted

aliphatic signal from lipids, amino acids and the *N*-acetyl group in peptidoglycan and chitin (Simpson et al. 2007) decreased with all the treatments. Signals from the α -protons in peptides increased with soil warming and decreased with N fertilization. Anomeric signals from peptides only increased in the heated soils while aromatic and amide signals increased with all the treatments. SOM constituents that exhibit a large degree of motion (diffusion) during acquisition are edited out of DE ^1H NMR spectra which highlight ^1H signals arising from relatively large macromolecular and/or rigid compounds only (Simpson et al. 2007). The DE ^1H NMR of the forest floor (Table S4 in ESM; Fig. 4) show that the relative intensity of the alkyl, *O*-alkyl, aromatic and amide signals are not attenuated suggesting that these structures are major constituents to the overall large/rigid structures. In the mineral soil the alkyl, aromatic and amide signals are not attenuated. The broad peak observed at 6.5 ppm in the DE ^1H NMR spectrum of the forest floor Control soil (Fig. 4) is an indicator of lignin presence (Woods et al. 2011). This lignin-derived signal is not as prominent in the spectrum of the mineral horizon Control soil and its absence suggests lignin degradation with soil depth. Major changes were not observed in the DE ^1H NMR of the forest floor and mineral soils with the different treatments.

2-D solution-state NMR for the confirmation of chemical shift assignments

Chemical shift assignments that were used to distinguish between plant- and microbial-derived inputs to base-soluble SOM extracts were confirmed by 2-D NMR techniques. A COSY experiment provides information on the connectivity between protons on neighboring carbons (Simpson et al. 2011). Figure 5a

shows the aliphatic and aromatic regions of the forest floor Control soil COSY NMR spectrum. The assignments within the aromatic region (Fig. 5b) are consistent with residues commonly found in lignin (Simpson et al. 2004). The acquisition of ^1H - ^{13}C HSQC NMR spectra facilitates the ^1H chemical shift assignments for 1-D experiments of base-soluble SOM extracts because of increased chemical shift dispersion of ^{13}C nuclei (Simpson et al. 2011).

Fig. 5 Examples of multidimensional NMR spectra of the forest floor Control soil. **a** Correlation spectroscopy (COSY); **b** expansion of the COSY aromatic region; **c** heteronuclear single quantum coherence (HSQC); **d** expansion of the HSQC aliphatic region; **e** heteronuclear multiple bond connectivity (HMBC); **f** expansion of the HMBC carboxylic acid region. The solid outline indicates the expanded region shown next to the corresponding full spectrum. Major peak assignments (Deshmukh et al. 2003, 2007; Simpson et al. 2004, 2007; Kelleher and Simpson 2006) are discussed in the text and in Table S5 in the ESM

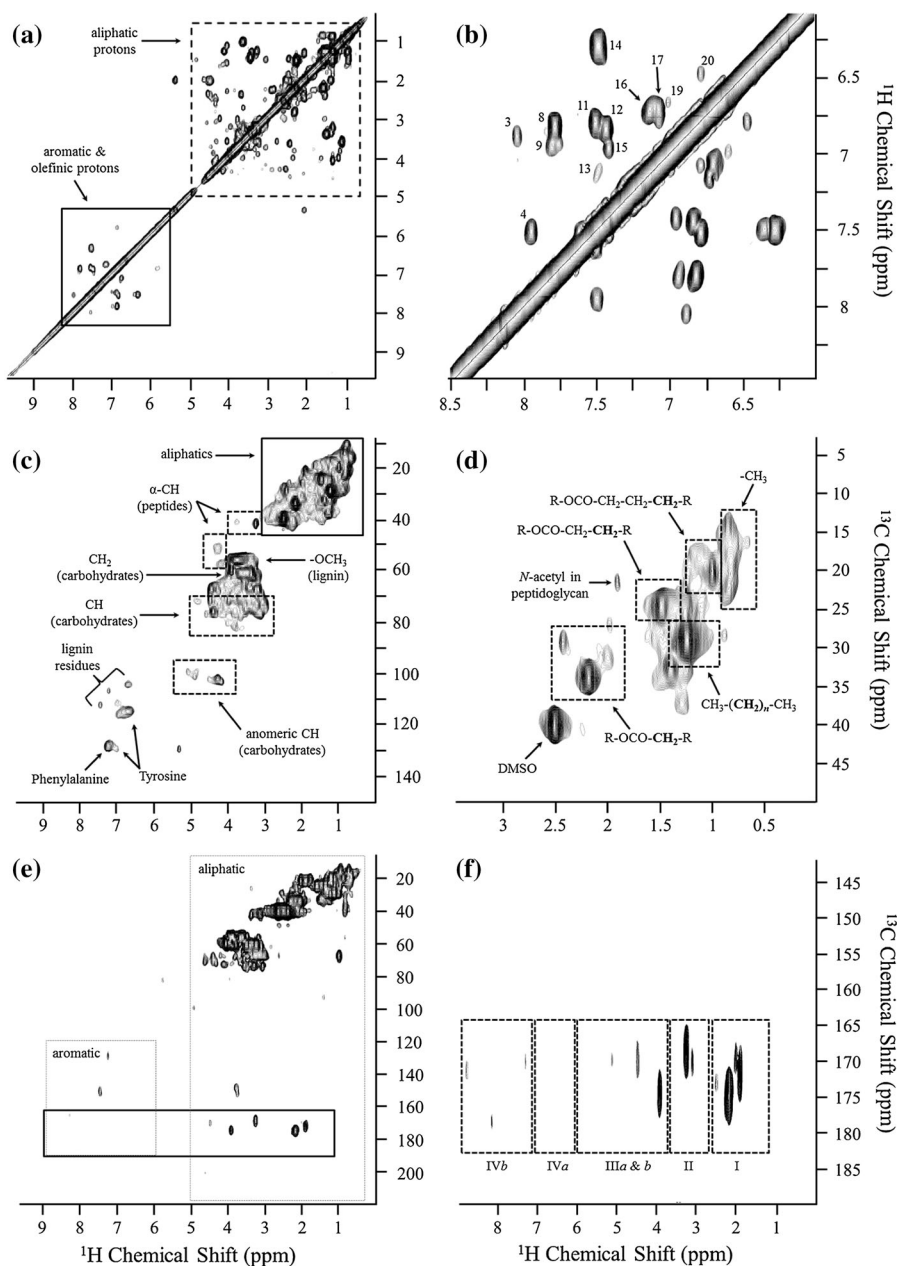


Figure 5c shows the major C–H couplings of plant-derived lignin and aliphatic groups as well as microbial protein/peptide amino acid side-chains and carbohydrates (Simpson et al. 2001, 2004; Deshmukh et al. 2003; Kelleher and Simpson 2006). Figure 5d is an expansion of the aliphatic region and shows signals from different aliphatic groups. The signal deriving from the *N*-acetyl functional group is of microbial origin and likely derives from peptidoglycan and/or chitin cell walls (Lorenz et al. 2007; Simpson et al. 2007). To assess changes in microbial and plant-derived signals with the different treatments, normalized area ratios were calculated by dividing the peak intensity by the total spectrum intensity (Pautler et al. 2010; Table S5 in ESM). In the forest floor soils, the signal originating from methylene groups derived from plant cutin and suberin (Deshmukh et al. 2003; Simpson et al. 2004) increased with both soil warming and N fertilization. However, the signal originating from the methoxyl group in lignin decreased with all the treatments. The microbial signal from the *N*-acetyl group in peptidoglycan or chitin and the anomeric CH from carbohydrates decreased in the N fertilized soils and in the soils receiving both treatments. The α -CH signal from peptides increased with all treatments. The signals originating from tyrosine and phenylalanine decreased in the heated and N fertilized soils, but increased with both treatments. The mineral horizon soils displayed a more intense methylene signal compared to the forest floor and this signal decreased in the heated and N fertilized soils. The signal from lignin was lower compared to the forest floor and also decreased with soil warming and N fertilization. The *N*-acetyl signal was more intense in the mineral soil and suggests the accumulation with soil depth. The normalized ratio of the *N*-acetyl group signal increased with all the treatments in the mineral soil. The α -CH in peptides increased with soil warming, but decreased with N fertilization. The signal from the anomeric CH in carbohydrates decreased with soil warming but increased with both treatments.

^1H – ^{13}C HMBC NMR spectra were also used to confirm the ^1H chemical shift assignments for 1-D experiments of base-soluble SOM extracts because HMBC experiments observe the coupling between protons and carbon atoms separated by 2–3 bonds (Deshmukh et al. 2007; Simpson et al. 2011). This type of experiment is particularly useful for probing carbons that are not directly bonded to protons such

as carboxyls and carbonyls (Deshmukh et al. 2007). Figure 5e shows the HMBC spectrum of the forest floor Control soil and highlights the regions of the spectrum dominated by aliphatic and aromatic components. Figure 5f is an expansion of the HMBC carboxylic acid region and the normalized area ratios for this region are summarized in Table S5 in ESM. The types of acids that can be identified using this technique include long-chain carboxylic acids, likely originating from cutin and suberin, as well as 5-(pyrroles and furans) and 6-membered heterocyclic aromatic acids (benzoic acid, salicylic acid and pyridine) which may originate from proteins or lignin (Deshmukh et al. 2007; Woods et al. 2011). The heteroatom-substituted and unsaturated acid region of the spectrum also contains contributions from uronic acids which can have multiple sources. In the forest floor samples, the aliphatic and alkyl-substituted long-chain carboxylic acids increased with soil warming, but decreased with N fertilization and with both treatments. The functionalized carbon-substituted long-chain carboxylic acids also increased with soil warming. The heteroatom-substituted and unsaturated long-chain carboxylic acids increased in the heated soils and increased slightly in the soils receiving both treatments. The 5- and 6-membered heterocyclic aromatic acids also increased in the heated soils. In the mineral soils, the normalized ratio of the aliphatic and alkyl-substituted, the functionalized carbon-substituted and the six-membered heterocyclic aromatic acids increased with all the treatments. The heteroatom-substituted and unsaturated acids decreased with all the treatments.

Discussion

Labile SOM components

Labile SOM components such as simple sugars and solvent-extractable SCA lipids increased in the forest floor with soil warming (Table S1 in ESM; Fig. 1b) likely due to enhanced vegetation productivity and litterfall that are predicted to occur with rising temperatures (Cramer et al. 2001; Liu et al. 2004). In a long-term soil warming experiment also conducted at the Harvard Forest, soil respiration decreased after 10 years of treatment and this was attributed to the limited size of the labile soil carbon pool (Melillo et al.

2002). This is consistent with the decline in labile constituents observed after 4 years of soil warming. The observed increase in gram-positive bacteria and actinomycetes (Table S1 in ESM), which was also observed after 12 years of soil warming at the Harvard Forest (Frey et al. 2008) indicates that increased microbial activity may be responsible for mediating soil priming (the enhanced decomposition of organic carbon upon addition of labile substrates; Kuzyakov et al. 2000) in the presence of labile carbon (Garcia-Pausas and Paterson 2011; Reinsch et al. 2013). The decrease in the concentration of cyclic compounds in the forest floor (Fig. 3a) is likely a result of soil priming and associated with increased activity of the soil microbial community. Interestingly, NMR analysis showed that *O*-alkyl components declined with soil warming, more so in the mineral horizon than in the forest floor, but not with N fertilization and with soil warming + N fertilization (Table S4 in ESM).

Four years of N fertilization to the forest floor also resulted in an increase in labile SCAs (Fig. 1b) which are likely plant-derived because the PLFA concentration did not increase. In the forest floor and mineral soils, the increase in solvent-extractable aliphatic and cyclic lipids (Fig. 3a, b) is likely due to an increase in plant productivity with N fertilization (Vitousek et al. 2002) or the suppression of microbial activity and SOM degradation (Frey et al. 2014). The accumulation of labile SOM (such as simple carbohydrates) in the mineral soils (Fig. 3b), is likely due to a decrease in microbial activity (decrease in total PLFAs) coupled with inputs of labile SOM via the translocation of dissolved organic matter from the forest floor above (Currie et al. 1996). As such, the suppression of microbial activity due to N fertilization has resulted in an accumulation of labile SOM components in the mineral horizon.

Under future climate change scenarios, soil warming and N fertilization are expected to occur simultaneously, but the influence of these combined factors on SOM composition and stage of degradation is still unclear (Pinder et al. 2012; Savage et al. 2013). In the Harvard Forest, the warmed + nitrogen forest floor and mineral soils showed enrichment in cyclic compounds and carbohydrates (Figs. 3e, f) suggesting increased fresh carbon inputs from the overlying vegetation. The accumulation of labile SOM components in the mineral warmed + nitrogen soils is also highlighted by a lower alkyl/*O*-alkyl ratio obtained

using ^{13}C NMR compared to the Control soil (Table S4 in ESM) which coincides with a decline in microbial activity (Table S1 in ESM). As observed with the N fertilization plots, the suppression of microbial activity may enhance labile SOM storage. Interestingly, soil warming coupled with N fertilization more closely mirrored the trends observed with N fertilization alone.

Lignin stability

Some studies have proposed that lignin may be stable in soils (Hedges and Mann 1979; Kögel-Knabner 2002; Melillo et al. 2002), but recent studies have shown that lignin may indeed be susceptible to soil priming brought on by environmental change or shifts in SOM composition (Feng et al. 2008, 2010; Crow et al. 2009; Pisani et al. 2013). Lignin concentration and oxidation stage in the forest floor soils varied with the different treatments. Enhanced lignin oxidation with N fertilization, albeit small, is reflected by the Ad/Al ratios of the lignin phenols (Fig. 2d). Fungi, which are the primary microbes involved in lignin depolymerisation and degradation (Hedges et al. 1988), had increased activity (as measured by PLFAs) with all the treatments, although these differences were not statistically significant and differed with each treatment (Table S1 in ESM). For example, the total concentration of lignin phenols (VSC) declined with N fertilization and in the warmed + nitrogen soils, but not with soil warming alone (Table S1 in ESM). Increased litterfall and soil warming may have increased dissolved organic matter transport to the mineral horizons where lignin oxidation was detected (discussed further in the next paragraph). With N fertilization, the concentration of cinnamyl and syringyl phenols declined (Table S1 in ESM) and is consistent with the relative recalcitrance of vanillyl phenols in soil environments (Hedges et al. 1988), suggesting that N fertilization accelerates lignin degradation in the forest floor preferentially. With 14 years of chronic N addition, in the Harvard Forest a reduction in phenol oxidase activity, an indicator of the lignin-degrading potential of the microbial community was observed (Frey et al. 2004). After 20 years of chronic N addition, Frey et al. (2014) reported higher rates of lignin accumulation using pyrolysis GC-MS. Our observations of enhanced lignin oxidation are consistent with other N fertilization studies

(Feng et al. 2010) and suggest that oxidized lignin may accumulate with N-amendment because of decreased microbial mineralization of lignin. This is also consistent with no observed differences in SOM composition with N fertilization by solid-state ^{13}C NMR. The solution-state ^1H NMR spectra, which are typically more resolved and able to detect subtle changes in SOM chemistry (Simpson et al. 2012; Clemente et al. 2012) show a small decrease in the aromatic signal intensity with N fertilization and in the warmed + nitrogen soils (Table S4 in ESM) and is consistent with a decline in the lignin phenol concentration (VSC). The DE ^1H NMR data reveal that macromolecular lignin components are consistent across all treatments (Table S4 in ESM) and supports the lignin phenol observations that identified evidence for lignin degradation but not to a great extent. The small decline in the methoxy signal intensity from HSQC NMR (Table S5 in ESM) further supports this hypothesis and suggests minor differences in side-chain cleavage of the lignin biopolymer and reflects different extents of lignin depolymerisation, the first step in the lignin decomposition process.

Lignin oxidation in the mineral soils was more pronounced than in the overlying forest floor, likely because of the lack of direct fresh plant inputs that makes it difficult to discern between fresh and previously deposited lignin in the forest floor. With soil warming and N fertilization, a decline in the total concentration of lignin phenols (VSC) was observed along with increased Ad/Al ratios (Table S1 in ESM; Fig. 2d) both of which are clear indicators of enhanced lignin oxidation. Soil warming also resulted in a decline in lignin dimer concentrations (Table S1 in ESM) suggesting that soil warming enhanced lignin degradation which is consistent with other reports for mineral soils (Feng et al. 2008). The solid-state ^{13}C NMR alkyl/O-alkyl ratio further supports the notion that soil warming enhanced the overall degradation of SOM (Table S4 in ESM). In the warmed + nitrogen soils, the VSC concentration was higher than the Control (Table S1 in ESM), but the Ad/Al ratios still reflected enhanced lignin oxidation (Fig. 2d). This may be due to enhanced plant productivity and dissolved organic matter translocation which introduced more total lignin into the mineral horizon and is consistent with the slight increase in the macromolecular aromatic signal observed by ^1H solution-state and DE ^1H solution-state NMR spectroscopy (Table S4 in

ESM) suggesting some lignin accumulation with the suppression of microbial activity (Frey et al. 2014). As with the forest floor samples, a large decline in soil aromaticity was not observed using NMR techniques but the 2-D methods again detected a decline in the methoxy signal intensity (Table S5 in ESM) which is indicative of lignin depolymerisation and degradation in the mineral soil horizons.

Accumulation of recalcitrant SOM

Plant-derived aliphatic compounds from cutin and suberin are believed to be more stable (Baldock et al. 1992; Riederer et al. 1993) and have been observed to accumulate in various types of environments (Nierop 1998; von Lützow et al. 2006; Lorenz et al. 2007; Pisani et al. 2014) and with short-term soil warming (Feng et al. 2008). In the Harvard Forest, soil warming enhanced cutin degradation in the forest floor (Fig. 2b), likely due to soil priming and shifts in the microbial community structure and activity. Suberin is believed to be more resistant to degradation than cutin because it is embedded in bark and root tissues of plants and contains a higher content of phenolic units (Riederer et al. 1993). In the forest floor, the total concentration of suberin-derived compounds increased with soil warming (Fig. 3a and HSQC NMR results in Table S5 in ESM), possibly due to increased belowground inputs or better preservation of this material compared to cutin. However, a significant decrease in the concentration of suberin- and cutin-derived compounds (Table S1 in ESM; Fig. 3b) and in the HSQC NMR methylene signal intensity (Table S5 in ESM) was observed in the mineral soils. This is likely due to an increase in plant productivity and fresh root inputs to the soil. With 4 years of soil warming, the microbial community likely utilized these more recalcitrant SOM components due to shifts in microbial utilization efficiency (Frey et al. 2013).

Fresh carbon inputs may enhance soil priming through an increased contribution of root-derived carbon (i.e., root exudates and rhizosphere organic matter; Crow et al. 2009). Four years of N fertilization caused enrichment of alkyl (Table S4 in ESM) and methylene structures (Table S5 in ESM) in the SOM base-soluble extracts. In the mineral soils, the decrease in suberin-derived compounds with N fertilization (Fig. 3b) may be caused by a shift in the microbial

community towards gram-negative bacteria (Table S1 in ESM) which have been reported to degrade labile material derived from root exudates (Treonis et al. 2004) and may in turn accelerate the degradation of these recalcitrant structures through soil priming. The enrichment in alkyl components (Table S4 in ESM) and plant-derived long-chain carboxylic acids (Table S5 in ESM) suggests the preservation of aliphatic structures in the base-soluble extracts of the mineral soils. These recalcitrant structures have been shown to accumulate in mineral soils of a temperate forest after 2 years of N fertilization (Feng et al. 2010). The combination of both treatments caused a decrease in the concentration of bound lipids in the forest floor (Table S1 in ESM), likely through soil priming. This is in agreement with the 2-D NMR results (Table S5 in ESM) which show a small reduction in the signal intensity derived from aliphatic structures in the base-soluble extracts of the forest floor SOM.

In addition to plant-derived aliphatic structures, microbial-derived carbon inputs to soils are now increasingly recognized as playing a far greater role in the stabilization of SOM than previously believed (Kiem and Kögel-Knabner 2003; Grandy and Neff 2008; Kindler et al. 2009; Miltner et al. 2009). The importance of microbes in SOM stabilization includes their ability to leave behind senesced biomass and to produce recalcitrant compounds that accumulate in soils. Microbial cell wall materials (peptidoglycan and chitin) are thought to be potentially important sources of carbon for long-term stabilization (Liang et al. 2011; Schimel and Schaeffer 2012). Peptidoglycan is a major component of bacterial cell walls comprising up to 50 % by weight of gram-positive bacteria (Kögel-Knabner 2002). This material can be protected from microbial degradation after cell death by copolymerization reactions and transformation, adding to the stable SOM pool (Kögel-Knabner 2002; Liang et al. 2011). Using HSQC NMR, we found that the intensity of the *N*-acetyl signal (Fig. 5d) increased in the heated and N fertilized mineral soils (Table S5 in ESM). Because the total soil microbial PLFAs decreased with these two treatments (Table S1 in ESM), the accumulation of *N*-acetyl in the mineral soils is most likely from the accumulation of dead or dormant bacteria (peptidoglycan) (Pautler et al. 2010) or fungi (chitin). These results suggest the accumulation of microbial-derived components may increase with chronic N fertilization.

Conclusions

To the best of our knowledge, this is the first study that combines two powerful molecular-level techniques (biomarkers and NMR methods) to determine the responses of SOM to rising temperature, N fertilization and both treatments. After 4 years of soil warming, N addition and soil warming + N addition, we observed distinct differences in the SOM composition. Consistent with our hypotheses, soil warming decreased labile SOM components and resulted in accelerated degradation of lignin and cutin. Soil warming likely stimulates the biodegradation of soil microbes which results in the enhanced degradation of more stable and recalcitrant forms of SOM. N fertilization did not markedly alter the SOM composition of the soil, likely through the suppression of microbial activity. However, we did observe some indication of slowed lignin degradation (oxidized lignin phenols along with intact macromolecular lignin by NMR) and the accumulation of microbial-derived cell wall components. When soil warming + N fertilization were combined, the results more closely mirrored those observed with N fertilization than soil warming alone. For instance, we observed the accumulation of labile SOM and more stable forms of SOM likely due to the decline in microbial activity. Interestingly, N amendment impacts on SOM superseded those observed with soil warming when the two treatments were performed simultaneously. These results suggest that future temperature increases and N deposition will control SOM decomposition patterns through changes in the soil microbial community and substrate utilization. Although we have identified molecular-level shifts in SOM composition with two important aspects of global environmental change, detailed comparisons with long-term studies combined with these molecular approaches will assist in the long-term elucidation of SOM biogeochemistry in forests.

Acknowledgments We thank two anonymous reviewers and the Associate Editor (Prof. Sharon Billings) for their helpful feedback on earlier versions of this manuscript. We also thank Melissa Knorr for sample collection and Jonathan Chio for assistance with the PLFA analysis. The Natural Sciences and Engineering Research Council (NSERC) of Canada is thanked for support via a Discovery Grant and a Discovery Accelerator Grant to M.J.S. Installation and maintenance of the Soil Warming × Nitrogen Addition Study at Harvard Forest was supported by a NSF Faculty Early Career Development Award to S.D.F. and the NSF Long-term Ecological Research (LTER) Program.

References

- Baldock JA, Skjemstad JO (2000) Role of the soil matrix and minerals in protecting natural organic materials against biological attack. *Org Geochem* 31:697–710
- Baldock JA, Oades JM, Waters AG, Peng X, Vassallo AM, Wilson MA (1992) Aspects of the chemical structure of soil organic materials as revealed by solid-state ^{13}C NMR spectroscopy. *Biogeochemistry* 16:1–42
- Batjes NH (1996) Total carbon and nitrogen in the soils of the world. *Eur J Soil Sci* 47:151–163
- Berg B, Berg MP, Bottner P, Box E, Breymeyer A, de Anta RC, Coûteaux MM, Gallardo A, Escudero A, Kratz W, Madeira M, Mälkönen E, Meentemeyer V, Munoz F, Piussi P, Remacle J, de Santo AV (1993) Litter mass loss rates in pine forests of Europe and Eastern United States: some relationships with climate and litter quality. *Biogeochemistry* 20:127–159
- Clemente JS, Gregorich EG, Simpson AJ, Kumar R, Courtier-Murias D, Simpson MJ (2012) Comparison of nuclear magnetic resonance methods for the analysis of organic matter composition from soil density and particle fractions. *Environ Chem* 9:97–107
- Conte P, Spaccini R, Piccolo A (2004) State of the art of CP/MAS ^{13}C -NMR spectroscopy applied to natural organic matter. *Prog Nucl Magn Reson Spectrosc* 44:215–223
- Contosta AR, Frey SD, Cooper AB (2011) Seasonal dynamics of soil respiration and N mineralization in chronically warmed and fertilized soils. *Ecosphere* 2(3):1–21 (article 36)
- Cramer W, Bondeau A, Woodward FI, Prentice IC, Betts RA, Brovkin V, Cox PM, Fisher V, Foley JA, Friend AD, Kucharik C, Lomas MR, Ramankutty N, Sitch S, Smith B, White A, Young-Molling C (2001) Global response of terrestrial ecosystem structure and function to CO_2 and climate changes: results from six dynamic global vegetation models. *Glob Change Biol* 7:357–373
- Crow SE, Lajtha K, Bowden RD, Yano Y, Brant JB, Caldwell BA, Sulzman EW (2009) Increased coniferous needle inputs accelerate decomposition of soil carbon in an old-growth forest. *For Ecol Manag* 258:2224–2232
- Currie WS, Aber JD, McDowell WH, Boone RD, Magill AH (1996) Vertical transport of dissolved organic C and N under long-term N amendments in pine and hardwood forests. *Biogeochemistry* 35:471–505
- Davidson EA, Janssens IA (2006) Temperature sensitivity of soil carbon decomposition and feedbacks to climate change. *Nature* 440:165–173
- Deshmukh AP, Simpson AJ, Hatcher PG (2003) Evidence for cross-linking in tomato cutin using HR-MAS NMR spectroscopy. *Phytochemistry* 64:1163–1170
- Deshmukh AP, Pacheco C, Hay MB, Myneni SCB (2007) Structural environments of carboxyl groups in natural organic molecules from terrestrial systems. Part 2: 2D NMR spectroscopy. *Geochim Cosmochim Acta* 71:3533–3544
- Feng X, Simpson MJ (2009) Temperature and substrate controls on microbial phospholipid fatty acid composition during incubation of grassland soils contrasting in organic matter quality. *Soil Biol Biochem* 41:804–812
- Feng X, Simpson MJ (2011) Molecular-level methods for monitoring soil organic matter responses to global climate change. *J Environ Monit* 13:1246–1254
- Feng X, Simpson AJ, Wilson KP, Williams DD, Simpson MJ (2008) Increased cuticular carbon sequestration and lignin oxidation in response to soil warming. *Nat Geosci* 1: 836–839
- Feng X, Simpson AJ, Schlesinger WH, Simpson MJ (2010) Altered microbial community structure and organic matter composition under elevated CO_2 and N fertilization in the duke forest. *Glob Change Biol* 16:2104–2116
- Frey SD, Knorr M, Parrent JL, Simpson RT (2004) Chronic nitrogen enrichment affects the structure and function of the soil microbial community in temperate hardwood and pine forests. *For Ecol Manag* 196:159–171
- Frey SD, Drijber R, Smith H, Melillo J (2008) Microbial biomass, functional capacity, and community structure after 12 years of soil warming. *Soil Biol Biochem* 40:2904–2907
- Frey SD, Lee J, Melillo JM, Six J (2013) The temperature response of soil microbial efficiency and its feedback to climate. *Nat Clim Change* 3:395–398
- Frey SD, Ollinger S, Nadelhoffer K, Bowden R, Brzostek E, Burton A, Caldwell BA, Crow S, Goodale CL, Grandy AS, Finzi A, Kramer MG, Lajtha K, LeMoine J, Martin M, McDowell WH, Minocha R, Sadowsky JJ, Templer PH, Wickings K (2014) Chronic nitrogen additions suppress decomposition and sequester soil carbon in temperate forests. *Biogeochemistry* 121(2):305–316
- Frostegård A, Bååth E (1996) The use of phospholipid fatty acid analysis to estimate bacterial and fungal biomass in soil. *Biol Fertil Soils* 22:59–65
- Galloway JN, Dentener FJ, Boyer EW, Capone DG, Howarth RW, Seitzinger SP, Asner GP, Cleveland CC, Green PA, Holland EA, Karl DM, Michaels AF, Porter JH, Townsend AR, Vörösmarty CJ (2004) Nitrogen cycles: past, present and future. *Biogeochemistry* 70:153–226
- García-Pausas J, Paterson E (2011) Microbial community abundance and structure are determinants of soil organic matter mineralisation in the presence of labile carbon. *Soil Biol Biochem* 43:1705–1713
- Goñi MA, Hedges JI (1990a) Cutin-derived CuO reaction products from purified cuticles and tree leaves. *Geochim Cosmochim Acta* 54:3065–3072
- Goñi MA, Hedges JI (1990b) The diagenetic behavior of cutin acids in buried conifer needles and sediments from a coastal marine environment. *Geochim Cosmochim Acta* 54:3083–3093
- Grandy AS, Neff JC (2008) Molecular C dynamics downstream: the biochemical decomposition sequence and its impact on soil organic matter structure and function. *Sci Total Environ* 404:297–307
- Guckert JB, Antworth CP, Nichols PD, White DC (1985) Phospholipid, ester-linked fatty acid profiles as reproducible assays for changes in prokaryotic community structure of estuarine sediments. *FEMS Microbiol Lett* 31:147–159
- Hedges JI, Mann DC (1979) The characterization of plant tissues by their lignin oxidation products. *Geochim Cosmochim Acta* 43:1803–1807

- Hedges JI, Blanchette RA, Weliky K, Devol AH (1988) Effects of fungal degradation on the CuO oxidation products of lignin: a controlled laboratory study. *Geochim Cosmochim Acta* 52:2717–2726
- IPCC (2007) Climate change 2007: synthesis report. An assessment of the intergovernmental panel on climate change. Intergovernmental Panel on Climate Change (IPCC), Valencia, Spain
- Kelleher BP, Simpson AJ (2006) Humic substances in soils: are they really chemically distinct? *Environ Sci Technol* 40:4605–4611
- Kiem R, Kögel-Knabner I (2003) Contribution of lignin and polysaccharides to the refractory carbon pool in C-depleted arable soils. *Soil Biol Biochem* 35:101–118
- Kindler R, Miltner A, Thullner M, Richnow HH, Kästner M (2009) Fate of bacterial biomass derived fatty acids in soil and their contribution to soil organic matter. *Org Geochem* 40:29–37
- Knorr M, Frey SD, Curtis PS (2005) Nitrogen additions and litter decomposition: a meta-analysis. *Ecology* 86:3252–3257
- Kögel-Knabner I (2002) The macromolecular organic composition of plant and microbial residues as inputs to soil organic matter. *Soil Biol Biochem* 34:139–162
- Kögel-Knabner I, Ekschmitt K, Flessa H, Guggenberger G, Matzner E, Marschner B, von Lütow M (2008) An integrative approach of organic matter stabilization in temperate soils: linking chemistry, physics and biology. *J Plant Nutr Soil Sci* 171:5–13
- Koide RT, Shumway DL, Stevens CM (2000) Soluble carbohydrates of red pine (*Pinus resinosa*) mycorrhizas and mycorrhizal fungi. *Mycol Res* 104:834–840
- Kolattukudy PE (1980) Biopolyester membranes of plants: cutin and suberin. *Science* 208:990–1000
- Kuzyakov Y, Friedel JK, Stahr K (2000) Review of mechanisms and quantification of priming effects. *Soil Biol Biochem* 32:1485–1498
- Lal R (2004) Soil carbon sequestration impacts on global climate change and food security. *Science* 304:1623–1627
- Lam TBT, Kadota K, Iiyama K (2001) Bonding of hydroxycinnamic acids to lignin: ferulic and *p*-coumaric acids are predominantly linked at the benzyl position of lignin, not the β -position, in grass cell walls. *Phytochemistry* 57:987–992
- Liang C, Cheng G, Wixon DL, Balsler TC (2011) An absorbing Markov chain approach to understanding the microbial role in soil carbon stabilization. *Biogeochemistry* 106:303–309
- Lichtfouse E, Berthier G, Houot S, Barriuso E, Bergheaud V, Vallaeyts T (1995) Stable carbon isotope evidence for the microbial origin of C₁₄–C₁₈ *n*-alkanoic acids in soils. *Org Geochem* 23:849–852
- Liu C, Westman CJ, Berg B, Kutsch W, Wang GZ, Man R, Ilvesniemi H (2004) Variation in litterfall–climate relationships between coniferous and broadleaf forests in Eurasia. *Global Ecol Biogeogr* 13:105–114
- Lorenz K, Lal R, Preston CM, Nierop KGJ (2007) Strengthening the soil organic carbon pool by increasing contributions from recalcitrant aliphatic bio(macro)molecules. *Geoderma* 142:1–10
- Mackenzie AS, Brassell SC, Eglinton G, Maxwell JR (1982) Chemical fossils: the geological fate of steroids. *Science* 217:491–504
- Melillo JM, Steudler PA, Aber JD, Newkirk K, Lux H, Bowles FP, Catricala C, Magill A, Ahrens T, Morrisseau S (2002) Soil warming and carbon-cycle feedbacks to the climate system. *Science* 298:2173–2176
- Melillo JM, Butler S, Johnson J, Mohan J, Steudler P, Lux H, Burrows E, Bowles F, Smith R, Scott L, Vario C, Hill T, Burton A, Zhou YM, Tang J (2011) Soil warming, carbon-nitrogen interactions, and forest carbon budgets. *Proc Natl Acad Sci* 108:9508–9512
- Miltner A, Kindler R, Knicker H, Richnow HH, Kästner M (2009) Fate of microbial biomass-derived amino acids in soil and their contribution to soil organic matter. *Org Geochem* 40:978–985
- Munger JW, Fan SM, Bakum PS, Goulden ML, Goldstein AH, Coleman AS, Wofsy SC (1998) Regional budgets for nitrogen oxides from continental sources: variations of rates for oxidation and deposition with season and distance from source regions. *J Geophys Res* 103:8355–8368
- Nierop KGJ (1998) Origin of aliphatic compounds in a forest soil. *Org Geochem* 29:1009–1016
- Otto A, Simpson MJ (2005) Degradation and preservation of vascular plant-derived biomarkers in grassland and forest soils from Western Canada. *Biogeochemistry* 74:377–409
- Otto A, Simpson MJ (2006a) Sources and composition of hydrolysable aliphatic lipids and phenols in soils from western Canada. *Org Geochem* 37:385–407
- Otto A, Simpson MJ (2006b) Evaluation of CuO oxidation parameters for determining the source and stage of lignin degradation in soil. *Biogeochemistry* 80:121–142
- Otto A, Simpson MJ (2007) Analysis of soil organic matter biomarkers by sequential chemical degradation and gas chromatography–mass spectrometry. *J Sep Sci* 30:272–282
- Pautler BG, Simpson AJ, McNally DJ, Lamoureux SF, Simpson MJ (2010) Arctic permafrost active layer detachments stimulate microbial activity and degradation of soil organic matter. *Environ Sci Technol* 44:4076–4082
- Pautler BG, Dubnick A, Sharp MJ, Simpson AJ, Simpson MJ (2013) Comparison of cryoconite organic matter composition from Arctic and Antarctic glaciers at the molecular-level. *Geochim Cosmochim Acta* 104:1–18
- Peterjohn WT, Mellor JM, Steudler PA, Newkirk KM, Bowles FP, Aber JD (1994) Responses of traces gas fluxes and N availability to experimentally elevated soil temperatures. *Ecol Appl* 4:617–625
- Pinder RW, Bettez ND, Bonan GB, Greaver TL, Wieder WR, Schlesinger WH, Davidson EA (2012) Impacts of human alteration of the nitrogen cycle in the US on radiative forcing. *Biogeochemistry* 114:25–40
- Pisani O, Hills KM, Courtier-Murias D, Simpson AJ, Mellor NJ, Paul EA, Morris SJ, Simpson MJ (2013) Molecular level analysis of longterm vegetative shifts and relationships to soil organic matter composition. *Org Geochem* 62:7–16
- Pisani O, Hills KM, Courtier-Murias D, Haddix ML, Paul EA, Conant RT, Simpson AJ, Arhonditsis GB, Simpson MJ (2014) Accumulation of aliphatic compounds in soil with increasing mean annual temperature. *Org Geochem* 76:118–127
- Reinsch S, Ambus P, Paterson E, Thornton B (2013) Impact of future climatic conditions on the potential for soil organic matter priming. *Soil Biol Biochem* 65:133–140

- Riederer M, Matzke Z, Ziegler F, Kögel-Knabner I (1993) Occurrence, distribution and fate of the lipid plant biopolymers cutin and suberin in temperate forest soils. *Org Geochem* 20:1063–1076
- Rumpel C, Rabia N, Derenne S, Quenea K, Eusterhues K, Kögel-Knabner I, Mariotti A (2006) Alteration of soil organic matter following treatment with hydrofluoric acid (HF). *Org Geochem* 37:1437–1451
- Savage KE, Parton WJ, Davidson EA, Trumbore SE, Frey SD (2013) Long-term changes in forest carbon under temperature and nitrogen amendments in a temperate northern hardwood forest. *Glob Change Biol* 19:2389–2400
- Schimel JP, Schaeffer SM (2012) Microbial control over carbon cycling in soil. *Front Microbiol*. doi:10.3389/fmicb.2012.00348
- Schlesinger WH, Andrews JA (2000) Soil respiration and the global carbon cycle. *Biogeochemistry* 48:7–20
- Schmidt MWI, Knicker H, Hatcher PG, Kögel-Knabner I (1997) Improvement of C-13 and N-15 CPMAS NMR spectra of bulk soils, particle size fractions and organic material by treatment with 10% hydrofluoric acid. *Europ J Soil Sci* 48:319–325
- Schmidt MWI, Torn MS, Abiven S, Dittmar T, Guggenberger G, Janssens IA, Kleber M, Kögel-Knabner I, Lehmann J, Manning DAC, Nannipieri P, Rasse DP, Weiner S, Trumbore SE (2011) Persistence of soil organic matter as an ecosystem property. *Nature* 478:49–56
- Schulten HR, Schnitzer M (1990) Aliphatics in soil organic matter in fine-clay fractions. *Soil Sci Soc Am J* 54:98–105
- Shaver GR, Canadell J, Chapin FS, Gurevitch J, Harte J, Henry G, Ineson P, Jonasson S, Melillo J, Pitelka L, Rustad L (2000) Global warming and terrestrial ecosystems: a conceptual framework for analysis. *BioScience* 50:871–882
- Simoneit BRT (2005) A review of current applications of mass spectrometry for biomarker/molecular tracer elucidations. *Mass Spectrom Rev* 24:719–765
- Simoneit BRT, Elias VO, Kobayashi M, Kawamura K, Rushdi AI, Medeiros PM, Rogge WF, Didyk BM (2004) Sugars-dominant water-soluble organic compounds in soils and characterization as tracers in atmospheric particulate matter. *Environ Sci Technol* 38:5939–5949
- Simpson MJ, Simpson AJ (2012) The chemical ecology of soil organic matter molecular constituents. *J Chem Ecol* 38:768–784
- Simpson AJ, Burdon J, Graham CL, Hayes MHB, Spencer N, Kingery WL (2001) Interpretation of heteronuclear and multidimensional NMR spectroscopy of humic substances. *Eur J Soil Sci* 52:495–509
- Simpson AJ, Lefebvre B, Moser A, Williams A, Larin N, Kvasha M, Kingery WL, Kelleher B (2004) Identifying residues in natural organic matter through spectral prediction and pattern matching of 2D NMR datasets. *Magn Reson Chem* 42:14–22
- Simpson AJ, Song G, Smith E, Lam B, Novotny EH, Hayes MHB (2007) Unraveling the structural components of soil humin by use of solution-state nuclear magnetic resonance spectroscopy. *Environ Sci Technol* 41:876–883
- Simpson MJ, Otto A, Feng X (2008) Comparison of solid-state carbon-13 nuclear magnetic resonance and organic matter biomarkers for assessing soil organic matter degradation. *Soil Sci Soc Am J* 72:268–276
- Simpson AJ, McNally DJ, Simpson MJ (2011) NMR spectroscopy in environmental research: from molecular interactions to global processes. *Prog Nucl Magn Reson Spectrosc* 58:97–175
- Simpson AJ, Simpson MJ, Soong R (2012) Nuclear magnetic resonance spectroscopy and its key role in environmental research. *Environ Sci Technol* 46:11488–11496
- Thenot JP, Horning EC, Stafford M, Horning MG (1972) Fatty acid esterification with N, N-Dimethylformamide dialkyl acetals for GC analysis. *Anal Lett* 5:217–223
- Treonis AM, Ostle NJ, Stott AW, Primrose R, Grayston SJ, Ineson P (2004) Identification of groups of metabolically-active rhizosphere microorganisms by stable isotope probing of PLFAs. *Soil Biol Biochem* 36:533–537
- Trumbore SE, Czimczik CI (2008) An uncertain future for soil carbon. *Science* 321:1455–1456
- Vitousek PM, Hättenschwiler S, Olander L, Allison S (2002) Nitrogen and nature. *Ambio* 31:97–101
- von Lützw M, Kögel-Knabner I, Ekschitt K, Matzner E, Guggenberger G, Marschner B, Flessa H (2006) Stabilization of organic matter in temperate soils: mechanisms and their relevance under different soil conditions—a review. *Eur J Soil Sci* 57:426–445
- Woods GC, Simpson MJ, Koerner PJ, Napoli A, Simpson AJ (2011) HILIC-NMR: toward the identification of individual molecular components in dissolved organic matter. *Environ Sci Technol* 45:3880–3886
- Zhang D, Hui D, Luo Y, Zhou G (2008) Rates of litter decomposition in terrestrial ecosystems: global patterns and controlling factors. *J Plant Ecol* 1:1–9